

Preparation, Structure, and Reactivity of Dipalladium(I) Complexes Containing the Carbanion 2-C₆F₄PPh₂: Coexistence of Distinct, Noninterconverting Head-to-Head [Dipalladium(0/II)] and Head-to-Tail [Dipalladium(I)] Species

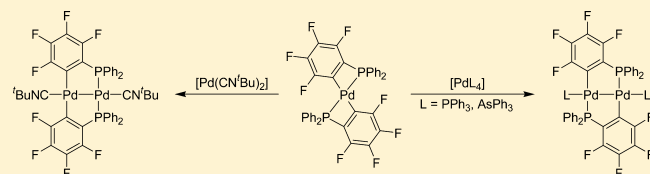
Suresh K. Bhargava,^{*,†} Steven H. Privér,[†] Anthony C. Willis,[‡] and Martin A. Bennett^{*,‡}

[†]School of Applied Sciences (Applied Chemistry), RMIT University, GPO Box 2476 V, Melbourne, Victoria 3001, Australia

[‡]Research School of Chemistry, Australian National University, Canberra, ACT 0200, Australia

Supporting Information

ABSTRACT: Comproportionation of *trans*-[Pd(κ^2 -2-C₆F₄PPh₂)₂] with [PdL₄] (L = PPh₃, AsPh₃) gives metal–metal-bonded dipalladium(I) complexes [Pd₂^I(μ -2-C₆F₄PPh₂)₂(L)₂] [L = PPh₃ (**5**), AsPh₃ (**6**)] in which the bridging ligands adopt a head-to-tail arrangement. The corresponding diplatinum(I) complex [Pt₂^I(μ -2-C₆F₄PPh₂)₂(PPh₃)₂] (**9**) is obtained similarly from [Pt(κ^2 -2-C₆F₄PPh₂)₂] and [Pt(PPh₃)₃]. The separations between the metal atoms in the dipalladium(I) complexes [2.5740(3) Å (**5**), 2.5511(3) Å (**6**)] are slightly less than that in the diplatinum(I) complex **9** [2.61179(15) Å]. The axial triphenylarsine ligands of **6** are replaced by *tert*-butyl isocyanide to give the dipalladium(I) complex [Pd₂^I(μ -2-C₆F₄PPh₂)₂(CN^tBu)₂] (**7**). However, treatment of *trans*-[Pd(κ^2 -2-C₆F₄PPh₂)₂] with [Pd(CN^tBu)₂], generated *in situ* from a mixture of *tert*-butyl isocyanide and [Pd(η^5 -Cp)(η^3 -allyl)], gives a formally mixed-valent palladium(0)–palladium(II) complex [Pd₂^{0/II}(μ -2-C₆F₄PPh₂)₂(CN^tBu)₂] (**8**), in which the bridging ligands are arranged head-to-head. In contrast, comproportionation of [Pt(κ^2 -2-C₆F₄PPh₂)₂] with [Pt₃(CN^tBu)₆] gives the diplatinum(I) complex [Pt₂^I(μ -2-C₆F₄PPh₂)₂(CN^tBu)₂] (**10**) analogous to **7**; there was no evidence for the formation of a dinuclear mixed-valent species. Although complexes **7** and **8** are isomers, with similar Pd–Pd separations [2.5803(4) Å (**7**), 2.5580(2) Å (**8**)], they do not interconvert in solution. The diplatinum(I) complex **9** undergoes oxidative addition with iodine to give an A-frame cation, [Pt₂(μ -I)(μ -2-C₆F₄PPh₂)₂(PPh₃)₂]⁺, isolated as its PF₆[−] salt (**11**). In contrast, the dipalladium(I) complex **5** eliminates one of the PPh₃ ligands when it undergoes oxidative addition with halogens and with methyl iodide, the products being A-frame dipalladium(II) complexes [Pd₂X(μ -Y)(μ -2-C₆F₄PPh₂)₂(PPh₃)₂] [X = Y = I (**12**), Cl (**13**); X = Me, Y = I (**14**)]. The metal–metal distances in **11**–**14** [2.9478(5) Å (**11**), 2.8078(7) Å (**12**), 2.8241(3) Å (**13**), and 2.8013(5) Å (**14**)] are ca. 0.3 Å greater than in their dimetal(I) precursors, consistent with a weaker metal–metal interaction in the dimetal(II) complexes. Unexpectedly, reaction of **5** with iodobenzene gives a mononuclear palladium(II) complex, *cis*-[Pd(κ^2 C,*P*-2-C₆F₄PPh₂)(κ C-2-C₆F₄PPh₂)(PPh₃)₂] (**15**). This is suggested to be formed by a sequence of (a) oxidative addition of iodobenzene to **5** to give a σ -phenyl complex analogous to the σ -methyl complex **14**, (b) a change in the binding mode of one of the 2-C₆F₄PPh₂ ligands from μ - to κ^2 -, and (c) reductive elimination of tetraphenylphosphonium iodide and loss of Pd(0).



INTRODUCTION

The *ortho*-C–H activation of triphenylphosphine is a well-established route to cyclometalated complexes of the d-block elements, although methods based on transmetalation from reagents such as 2-LiC₆H₄PPh₂ and on oxidative addition of 2-BrC₆H₄PPh₂ have also found application.¹ Most of the resulting complexes are mononuclear and contain the four-membered ring M(κ^2 C,*P*-2-C₆H₄PPh₂); however, there are cases where, in the reaction product, the carbanion functions as a bridging, bidentate ligand. Examples are [Rh₂(MeCO₂H)₂(μ -O₂CMe)₂(μ -2-C₆H₄PPh₂)₂], which is isolated from the reaction of dirhodium(II) tetraacetate with PPh₃ in glacial acetic acid,² and [Pt₂(μ -PPh₂)(μ -2-C₆H₄PPh₂)(PPh₃)₂], which is one of the products of thermal decomposition of platinum(0)-triphenylphosphine complexes.^{3,4} Interconversion between the two binding modes has also been demonstrated.

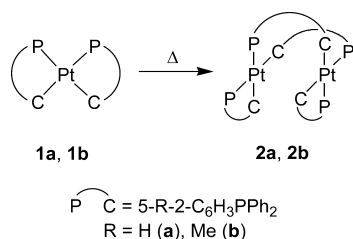
For example, the mononuclear platinum(II) complexes *cis*-[Pt(κ^2 C,*P*-5-R-2-C₆H₃PPh₂)₂] [R = H (**1a**), Me (**1b**)] dimerize on heating to diplatinum(II) complexes **2a** and **2b** (Scheme 1),^{5,6} and the tetrapalladium(II) complex [Pd₄(μ -Br)₄(μ -2-C₆H₄PPh₂)₄] (**3**) reacts with moderately bulky tertiary phosphines to give monomeric species [PdBr(κ^2 C,*P*-C₆H₄PPh₂)(L)] (L = PPh₃, PCy₃) (Scheme 2).^{7,8}

Comproportionation of the platinum(II) complex **1a** or **1b** with [Pt(PPh₃)₃] affords diplatinum(I) complexes [Pt₂(μ -5-R-2-C₆H₃PPh₂)₂(PPh₃)₂] [R = H (**3a**), Me (**3b**)], in which the carbanions bridge, in a head-to-tail (HT) arrangement, a pair of covalently bound platinum(I) (5d⁹) atoms (Scheme 3).^{5,6} Efforts to extend these studies to the corresponding

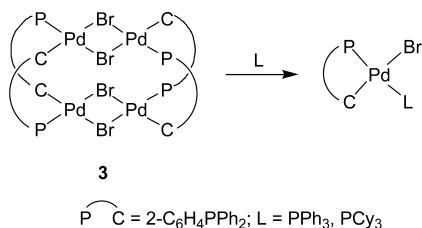
Received: June 12, 2012

Published: August 1, 2012

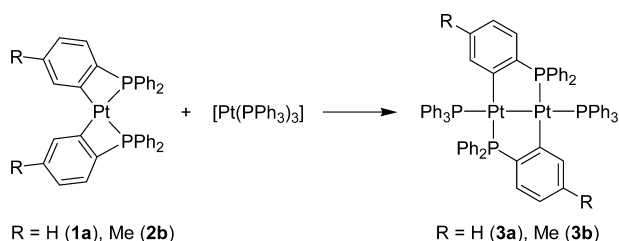
Scheme 1



Scheme 2



Scheme 3

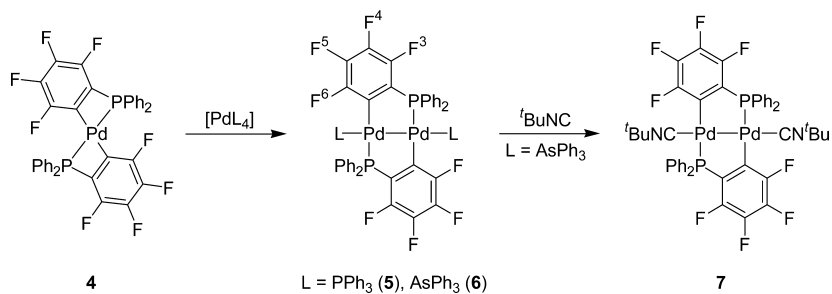


dipalladium(I) complexes have been frustrated by our inability thus far to make the palladium(II) analogues of **1a** and **1b**. Nevertheless, we have made a stable *ortho*-palladated complex, *trans*-[Pd(κ^2 -2-C₆F₄PPh₂)₂] (**4**),⁹ thus exemplifying the stabilization of transition metal–aryl bonds (especially those of palladium)¹⁰ brought about by the substitution of hydrogen by fluorine in the aromatic ring. We show here that complex **4** is a suitable precursor to *ortho*-metalated dipalladium(I) species and compare some of their chemistry with that of the corresponding diplatinum(I) compound.

RESULTS

Dipalladium(I) Complexes. Comproportionation of *trans*-[Pd(κ^2 -2-C₆F₄PPh₂)₂] (**4**) with [Pd(PPh₃)₄] at room temperature, or with [Pd(AsPh₃)₄] at 60 °C, gave the dipalladium(I) complexes [Pd₂^I(μ -2-C₆F₄PPh₂)₂(L)₂] [L = PPh₃ (**5**), AsPh₃ (**6**)] as orange and yellow solids, respectively, in 80–95% yield (Scheme 4). Complex **5** could also be prepared from the

Scheme 4

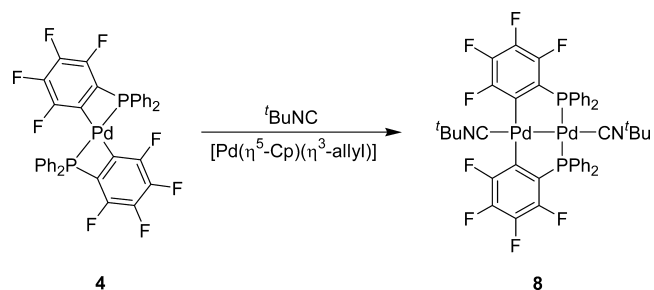


reaction of **4** with PPh₃ and [Pd(η^5 -Cp)(η^3 -allyl)] at low temperature. Complexes **5** and **6** gave satisfactory elemental analyses, and their ESI mass spectra each showed a peak corresponding to the [M]⁺ ion. The Raman spectra of both compounds displayed a strong band at ca. 130 cm⁻¹, assigned to $\nu(\text{Pd-Pd})$, the value being similar to those reported for the bis(diphenylphosphino)methane (dppm)-bridged dipalladium(I) complexes [Pd₂X₂(μ -dppm)₂] (X = Cl, 152 cm⁻¹; X = Br, 120 cm⁻¹).¹¹ The ³¹P NMR spectrum of **5** contained two resonances at δ -19.3 and 8.4, corresponding to the phosphorus nuclei in the bridging and axial ligands, respectively; that of **6** showed only one broad resonance at δ -17.6, assigned to the bridging 2-C₆F₄PPh₂ groups. The ¹⁹F NMR spectra of **5** and **6** showed the expected four resonances, at ca. δ -105, -130, -153, and -163 ppm relative to CFCl₃. By analogy with the previously reported spectra of 2-C₆F₄PPh₂ complexes of Pd and Pt,⁹ we assign these to F⁶ (*ortho* to Pd-C), F³ (*ortho* to PPh₂), and F⁵ and F⁴ (*para* to Pd-C), respectively (numbering shown in Scheme 4). The structures proposed for **5** and **6** have been confirmed by X-ray crystallography (see later).

Attempts to produce heterobimetallic complexes by comproportionation of [Pt(κ^2 -2-C₆F₄PPh₂)₂] with [Pd(PPh₃)₄], or of complex **4** with [Pt(PPh₃)₃], were unsuccessful.

When a solution of complex **6** was treated with two equivalents of *tert*-butyl isocyanide, the axial triphenylarsine ligands were displaced to give the dipalladium(I) complex [Pd₂^I(μ -2-C₆F₄PPh₂)₂(CN^{*t*}Bu)₂] (**7**) (Scheme 4), which was isolated as a yellow solid in 91% yield. Surprisingly, when a solution of *trans*-[Pd(κ^2 -2-C₆F₄PPh₂)₂] (**4**) was treated sequentially with *t*BuNC and [Pd(η^5 -Cp)(η^3 -allyl)], providing [Pd(CN^{*t*}Bu)₂] *in situ*,¹² the product isolated was not **7** but the isomeric, pale yellow, mixed-valent complex [Pd₂^{0/II}(μ -2-C₆F₄PPh₂)₂(CN^{*t*}Bu)₂] (**8**), in which, as shown by X-ray crystallography (see later), the bridging 2-C₆F₄PPh₂ groups are arranged head-to-head (HH) (Scheme 5). In addition to the

Scheme 5



expected aromatic multiplets, the ^1H NMR spectrum of **7** shows a singlet at δ 0.56 due to the equivalent protons of the $^t\text{BuNC}$ ligands, whereas the spectrum of **8** contains a pair of singlets of equal intensity at δ 0.45 and 0.63, demonstrating the inequivalence of the $^t\text{BuNC}$ ligands in **8**. The ^{19}F NMR spectra of **7** and **8** are similar to those of **4–6**, although the resonances due to the *ortho*-fluorine atoms (F^6) are shifted from ca. δ -105 to -109 in the case of **7** and -113 in the case of **8**, possibly because F^6 resides in the shielding zone of the $\text{N}\equiv\text{C}$ groups. The ^{31}P NMR spectra of **7** and **8** each show a broad singlet at ca. δ -14 , consistent with the presence of equivalent μ -2- $\text{C}_6\text{F}_4\text{PPh}_2$ groups, and the ESI mass spectra both have a parent-ion peak at m/z 1046. The IR spectrum of **7** in a KBr disk shows a strong $\nu(\text{N}\equiv\text{C})$ band at 2164 cm^{-1} , whereas the spectrum of **8** in Nujol shows two such bands, at 2159 and 2187 cm^{-1} , again consistent with the presence of inequivalent $^t\text{BuNC}$ groups. There was no evidence from the ^{31}P NMR spectra for interconversion of these HH and HT isomers in air- and moisture-free dichloromethane at room temperature; decomposition occurred on heating.

To enable direct comparison between analogous 4d^9 – 4d^9 and 5d^9 – 5d^9 systems, we prepared the dipalladium(I) analogues of complexes **5** and **7**, $[\text{Pd}_2^{\text{I}}(\mu\text{-}2\text{-C}_6\text{F}_4\text{PPh}_2)_2(\text{L})_2]$ [$\text{L} = \text{PPh}_3$ (**9**), $^t\text{BuNC}$ (**10**)], by the comproportionation of $[\text{Pt}(\kappa^2\text{-}2\text{-C}_6\text{F}_4\text{PPh}_2)_2]$ with $[\text{Pt}(\text{PPh}_3)_3]$ and $[\text{Pt}_3(\text{CN}^t\text{Bu})_6]$, respectively. The ESI mass spectra of **9** and **10** each showed a peak corresponding to $[\text{M} + \text{H}]^+$, and the Raman spectrum of **9** displayed a strong band at 126 cm^{-1} assignable to $\nu(\text{Pt}\text{--}\text{Pt})$, cf., 150 cm^{-1} in $[\text{Pt}_2\text{Cl}_2(\mu\text{-dppm})_2]$,¹³ 157 cm^{-1} in $[\text{Pt}_2\text{Cl}(\text{CO})(\mu\text{-dppm})_2]\text{PF}_6$,¹⁴ and 165 cm^{-1} in $[\text{Pt}_2(\text{CO})_6]^{2+}$;¹⁵ the corresponding band in **10** was not observed. The ^{31}P NMR spectrum of **9** contained a pair of resonances at δ -8.2 and 24.4 due to the phosphorus nuclei in the 2- $\text{C}_6\text{F}_4\text{PPh}_2$ (P_A) and axial PPh_3 (P_B) ligands, respectively, together with complex platinum satellites. Simulation of the AA'BB'XX' spin system (ignoring ^{19}F coupling) enabled extraction of the P–P and Pt–P coupling constants (see Experimental Section), which are, in general, similar to those for complexes **3a** and **3b**.^{5,6} One notable difference appears in the values of $^1J_{\text{PtP}}$ (J_{AX}), which are 2369 Hz for **9**, 1937 Hz for **3a**, and 1918 Hz for **3b**, the larger value for **9** being consistent with the lower NMR *trans* influence of the perfluoroaryl group.¹⁶ In addition, the magnitude of the coupling constant between the phosphorus nuclei of the bridging groups ($J_{\text{AA}'}$) appears to be close to zero in **9**, in contrast to ca. 55 Hz in **3a** and **3b**. The ^{31}P NMR spectrum of **10** showed a broad singlet at δ -7.4 . Simulation of the AA'XX' spin system gave ^{195}Pt coupling constants of 2330 Hz (J_{AX}) and 156 Hz ($J_{\text{AX}'}$), which are comparable to the corresponding values in **9** (2369 and 133 Hz , respectively). As was observed in **9**, the magnitude of the coupling between the two phosphorus nuclei in **10** appears to be close to zero; however, both spectra are complicated by unresolved ^{19}F coupling to P_A , which may lead to errors in the estimated values of $J_{\text{AA}'}$.

The ^{19}F NMR spectra of **9** and **10** are similar to those of the dipalladium(I) complexes **6** and **7**, the resonance due to F^6 at ca. δ -105 being accompanied by ^{195}Pt satellites [$^3J_{\text{PtF}} = 267\text{ Hz}$ (**9**), 262 Hz (**10**)]. The magnitudes of these coupling constants are comparable with the values of $^3J_{\text{PtF}}$ in *cis*- $[\text{Pt}(\text{C}_6\text{F}_5)_2(\text{L})_2]$ [$\text{L}_2 = 2\text{PPh}_3$ (315 Hz),¹⁷ *dppe* (309 Hz)¹⁸].

X-ray Structures of the Dipalladium(I), Palladium(0)–Palladium(II), and Diplatinum(I) Complexes. Single-crystal X-ray structural analyses have been carried out on $[\text{Pd}_2^{\text{I}}(\mu\text{-}2\text{-C}_6\text{F}_4\text{PPh}_2)_2(\text{L})_2]$ [$\text{L} = \text{PPh}_3$ (**5**), AsPh_3 (**6**), $^t\text{BuNC}$ (**7**)], $[\text{Pd}_2^{0/\text{II}}(\mu\text{-}2\text{-C}_6\text{F}_4\text{PPh}_2)_2(\text{CN}^t\text{Bu})_2]$ (**8**), and $[\text{Pt}_2^{\text{I}}(\mu\text{-}2\text{-C}_6\text{F}_4\text{PPh}_2)_2(\text{L})_2]$ [$\text{L} = \text{PPh}_3$ (**9**), $^t\text{BuNC}$ (**10**)]. The crystals of **5** and **6** were isomorphous with that of **9** (monoclinic, $\text{P}2_1/n$). The molecular structures of **7–9** are shown in Figures 1–3, respectively; selected bond distances and angles for **5–7**, **9**, and **10** are collected in Table 1, and selected bond distances and angles for **8** are shown in the caption to Figure 2.

$\text{C}_6\text{F}_4\text{PPh}_2)_2(\text{L})_2]$ [$\text{L} = \text{PPh}_3$ (**5**), AsPh_3 (**6**), $^t\text{BuNC}$ (**7**)], $[\text{Pd}_2^{0/\text{II}}(\mu\text{-}2\text{-C}_6\text{F}_4\text{PPh}_2)_2(\text{CN}^t\text{Bu})_2]$ (**8**), and $[\text{Pt}_2^{\text{I}}(\mu\text{-}2\text{-C}_6\text{F}_4\text{PPh}_2)_2(\text{L})_2]$ [$\text{L} = \text{PPh}_3$ (**9**), $^t\text{BuNC}$ (**10**)]. The crystals of **5** and **6** were isomorphous with that of **9** (monoclinic, $\text{P}2_1/n$). The molecular structures of **7–9** are shown in Figures 1–3, respectively; selected bond distances and angles for **5–7**, **9**, and **10** are collected in Table 1, and selected bond distances and angles for **8** are shown in the caption to Figure 2.

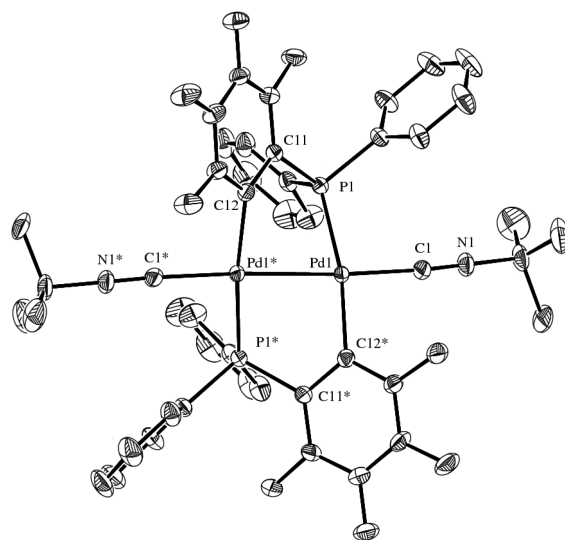


Figure 1. Molecular structure of $[\text{Pd}_2^{\text{I}}(\mu\text{-}2\text{-C}_6\text{F}_4\text{PPh}_2)_2(\text{CN}^t\text{Bu})_2]$ (**7**) with selected atom labeling. Ellipsoids show 30% probability levels, and asterisks denote atoms generated by symmetry. Hydrogen atoms have been omitted for clarity.

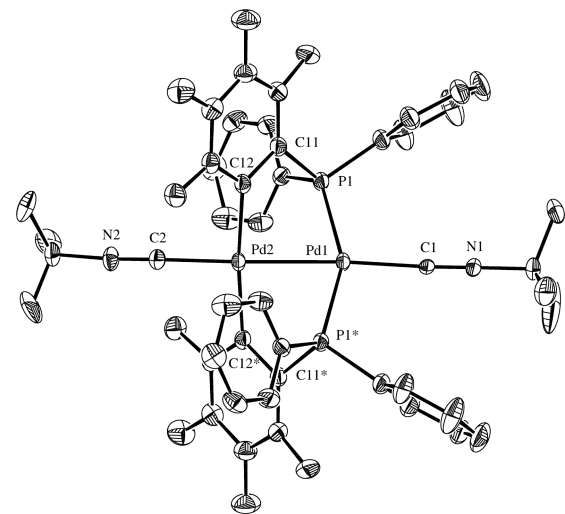


Figure 2. Molecular structure of $[\text{Pd}_2^{0/\text{II}}(\mu\text{-}2\text{-C}_6\text{F}_4\text{PPh}_2)_2(\text{CN}^t\text{Bu})_2]$ (**8**) with selected atom labeling. Ellipsoids show 30% probability levels, and asterisks denote atoms generated by symmetry. Hydrogen atoms have been omitted for clarity. Selected bond distances (Å) and angles (deg): Pd(1)–Pd(2) 2.5580(2), Pd(1)–P(1) 2.3013(5), Pd(1)–C(1) 2.057(3), Pd(2)–C(2) 1.993(3), Pd(2)–C(12) 2.076(2), Pd(2)–Pd(1)–P(1) 76.461(13), P(1)–Pd(1)–C(1) 108.15(19), P(1)–Pd(1)–P(1*) 152.92(3), Pd(2)–Pd(1)–C(1) 175.2(2), Pd(1)–Pd(2)–C(12) 87.08(5), C(2)–Pd(2)–C(12) 93.0(4), C(12)–Pd(2)–C(12*) 174.17(11), Pd(1)–Pd(2)–C(2) 175.6(5).

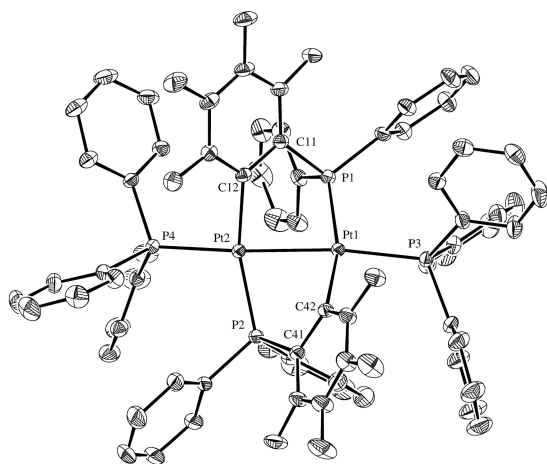


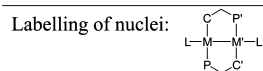
Figure 3. Molecular structure of $[\text{Pt}_2^{\text{I}}(\mu\text{-}2\text{-C}_6\text{F}_4\text{PPh}_2)_2(\text{PPh}_3)_2]$ (**9**) with selected atom labeling. Ellipsoids show 30% probability levels, and hydrogen atoms have been omitted for clarity.

The structures of **5**–**7**, **9**, and **10** resemble those of the corresponding diplatinum(I) complexes of $\mu\text{-}2\text{-C}_6\text{H}_4\text{PPh}_2$ (**3a**) and $\mu\text{-}5\text{-Me-}2\text{-C}_6\text{H}_3\text{PPh}_2$ (**3b**)^{5,6} and consist of two directly bonded metal atoms bridged by the carbanions in a head-to-tail arrangement. Distorted planar coordination about the metal atoms is completed by the axial ligands (PPh_3 for **5** and **9**, AsPh_3 for **6** and $^t\text{BuNC}$ for **7** and **10**) that are *trans* to the metal–metal bond, the L-M-M-L units being close to linear. The Pt–Pt bond length in **10** [2.5941(2) Å] is slightly shorter than that in **9** [2.61179(5) Å], consistent with the higher *trans* influence of the P-donor ligand, and is comparable to those in **3a** and **3b** [2.630(1), 2.61762(16) Å], respectively. The Pd–Pd distances are ca. 0.04 Å less than these and increase in the order $\text{L} = \text{AsPh}_3$ (**6**) < PPh_3 (**5**) < $^t\text{BuNC}$ (**7**), which does not correspond with the order of increasing *trans* influence of these ligands. A noteworthy feature is that both the M–P and M–C bond lengths in the diplatinum(I) complex **9** are less than those in its dipalladium(I) analogue **5**, by ca. 0.03–0.05 Å (M–P) and ca. 0.01 Å (M–C). A similar trend is observed for the M–P distances in the divalent metal complexes *cis*- $[\text{MMe}_2(\text{PMePh}_2)_2]$ ($\text{M} = \text{Pt}, \text{Pd}$), whereas the M–C distances show the opposite trend.^{19,20} In the $^t\text{BuNC}$ complexes, the M–P bond lengths in **10** are ca. 0.02 Å shorter than those in its palladium analogue **7**; the M–C bond lengths are comparable.

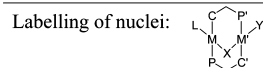
The X-ray structural analysis of complex **8** confirms the conclusion drawn from NMR and IR spectra that the $\mu\text{-}2\text{-C}_6\text{F}_4\text{PPh}_2$ groups are arranged head-to-head. Selected bond distances and angles are given in the caption to Figure 2. As is true also for complex **7**, the methyl groups of the $^t\text{BuNC}$ ligands are disordered, and only one location for these groups is shown. The Pd⋯Pd separation in **8** [2.5580(2) Å] is slightly less than that in **7**, whereas the Pd–P distance in **8** is about 0.03 Å greater than that in **7**; the Pd–C(aryl) distances are equal. The Pd–C bond lengths to the axial $^t\text{BuNC}$ ligands are significantly different [Pd(1)–C(1) = 2.057(3) Å, Pd(2)–C(2) = 1.993(3) Å], the shorter distance being to the formally divalent metal atom. The corresponding bond length in **7** is midway between these values. Moreover, whereas the coordination geometry about Pd(2) is close to planar, as expected [C(12)–Pd(2)–C(12*) = 174°, Pd(1)–Pd(2)–C(2) = 176°], that about Pd(1) is markedly distorted from planarity [P(1)–Pd(1)–P(1*) = 153°, Pd(2)–Pd(1)–C(1) = 175°]. This distortion may reflect the attempt of the d¹⁰ metal center

Table 1. Selected Bond Distances (Å) and Angles (deg) for $[\text{Pd}_2^{\text{I}}(\mu\text{-}2\text{-C}_6\text{F}_4\text{PPh}_2)_2(\text{L})_2]$ [$\text{L} = \text{PPh}_3$ (**5**), AsPh_3 (**6**), $^t\text{BuNC}$ (**7**)], $[\text{Pt}_2^{\text{I}}(\mu\text{-}2\text{-C}_6\text{F}_4\text{PPh}_2)_2(\text{L})_2]$ [$\text{L} = \text{PPh}_3$ (**9**), $^t\text{BuNC}$ (**10**)], $[\text{Pt}_2(\mu\text{-I})(\mu\text{-}2\text{-C}_6\text{F}_4\text{PPh}_2)_2(\text{PPh}_3)_2][\text{PF}_6]$ (**11**), and $[\text{Pd}_2\text{Y}(\mu\text{-X})(\mu\text{-}2\text{-C}_6\text{F}_4\text{PPh}_2)_2(\text{PPh}_3)]$ [$\text{X} = \text{Y} = \text{I}$ (**12**), Cl (**13**); $\text{X} = \text{I}$, $\text{Y} = \text{Me}$ (**14**)]

	5	6	7	9	10
M–M'	2.5740(3)	2.5511(3)	2.5803(4)	2.61179(15)	2.5941(2)
M–P	2.3232(7)	2.3127(9)	2.2748(8)	2.2921(7)	2.2586(8)
M'–P'	2.3255(7)	2.3205(9)		2.2932(8)	2.2526(8)
M–C	2.078(3)	2.067(3)	2.076(3)	2.069(3)	2.076(3)
M'–C'	2.056(3)	2.055(3)		2.048(3)	2.074(3)
M–L	2.3696(7)	2.4736(4)	2.029(3)	2.3198(8)	1.983(3)
M'–L'	2.3607(8)	2.4649(4)		2.3154(8)	1.979(3)
L–M–C	95.32(8)	94.43(9)	89.63(8)	94.49(9)	92.32(12)
M'–M–P	80.662(19)	80.99(2)	81.54(2)	80.33(2)	81.58(2)
P–M–C	161.62(8)	164.00(9)	169.62(9)	162.88(9)	170.72(9)
P'–M'–C'	162.77(8)	163.94(9)		163.66(9)	170.39(9)
M'–M–L	171.63(2)	171.679(15)	175.24(10)	172.04(2)	177.10(8)



	11^a	12^b	13^c	14^d
M'–M'	2.9478(5)	2.8078(7)	2.8241(3)	2.8013(5)
M–P	2.355(3)	2.4264(17)	2.3999(7)	2.4396(15)
M'–P'	2.364(2)	2.3535(18)	2.3550(7)	2.2959(14)
M–C	2.069(9)	2.049(6)	2.033(2)	2.053(5)
M'–C'	2.068(9)	2.030(7)	2.032(3)	2.046(5)
M–X	2.7115(7)	2.7090(6)	2.4261(6)	2.7101(5)
M–L	2.309(2)	2.3327(17)	2.2760(6)	2.3028(13)
M'–X	2.7035(7)	2.6529(7)	2.3507(6)	2.7386(5)
M'–Y	2.302(2)	2.5995(7)	2.3201(7)	2.162(4)
M–X–M'	65.964(17)	63.144(18)	72.466(18)	61.876(13)
P–M–C	171.5(3)	172.16(19)	169.53(7)	172.69(14)
P'–M'–C'	171.5(3)	175.1(2)	175.40(8)	177.11(13)
L–M–X	158.28(7)	166.77(5)	172.36(2)	166.38(4)
Y–M'–X	158.50(6)	170.22(3)	175.99(3)	173.68(11)

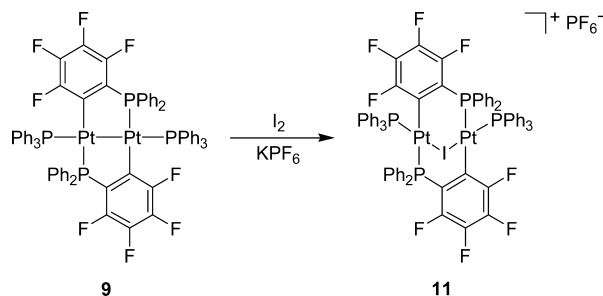


^a $\text{M} = \text{Pt}$, $\text{X} = \text{PPh}_3$, $\text{Y} = \text{I}$. ^b $\text{M} = \text{Pd}$, $\text{X} = \text{Y} = \text{I}$. ^c $\text{M} = \text{Pd}$, $\text{X} = \text{Y} = \text{Cl}$, one of the two independent molecules in the asymmetric unit. ^d $\text{M} = \text{Pd}$, $\text{X} = \text{I}$, $\text{Y} = \text{Me}$.

to achieve its favored trigonal-planar coordination, as observed, for example, in $[\text{Pt}(\text{PPh}_3)_3]$,^{21–23} this tendency being opposed by the presence of the adjacent metal atom and its associated ligands.

Reactions. 1. Diplatinum(I). Like its $\mu\text{-}2\text{-C}_6\text{H}_4\text{PPh}_2$ and $\mu\text{-}5\text{-Me-}2\text{-C}_6\text{H}_3\text{PPh}_2$ analogues,^{5,6} the diplatinum(I) complex **9** underwent oxidative addition with iodine to give the expected A-frame cation $[\text{Pt}_2(\mu\text{-I})(\mu\text{-}2\text{-C}_6\text{F}_4\text{PPh}_2)_2(\text{PPh}_3)_2]^+$, isolated as its PF_6^- salt (**11**) (Scheme 6). The ³¹P NMR spectrum of **11**

Scheme 6



shows a pair of broad, unresolved multiplets at δ 4.4 and 10.3, flanked by ^{195}Pt satellites, due to the bridging 2- $\text{C}_6\text{F}_4\text{PPh}_2$ (P_A) and axial PPh_3 (P_B) ligands, respectively. The derived coupling constants (see Experimental Section) are generally similar to those of the corresponding μ -2- $\text{C}_6\text{H}_4\text{PPh}_2$ and μ -5-Me-2- $\text{C}_6\text{H}_3\text{PPh}_2$ compounds, although some of the coupling constants could not be determined because of unresolved ^{19}F coupling. The bridging iodide ligand between the two platinum atoms causes a large increase in the magnitude of J_{BX} ($\text{X} = ^{195}\text{Pt}$) from 2001 Hz in **9** to 4645 Hz, cf. values of ca. 5080 Hz in $[\text{Pt}_2(\mu\text{-I})(\mu\text{-5-R-2-C}_6\text{H}_3\text{PPh}_2)_2]^+$ ($\text{R} = \text{H, Me}$)^{5,6} and 4265 Hz in $[\text{Pt}_2(\mu\text{-S})(\mu\text{-I})(\text{PPh}_3)_4]^+$;²⁴ disruption of the Pt–Pt bond is also responsible for the reduction of the long-range J_{BX} coupling from 904 to 128 Hz. The ^{19}F NMR spectrum of **11**, like that of its precursor **9**, shows the expected four resonances arising from the equivalent 2- $\text{C}_6\text{F}_4\text{PPh}_2$ groups, and the Raman spectrum contains a strong band at 154 cm^{-1} assignable to $\nu(\text{Pt}\text{--I})$.²⁵ The molecular structure of the cation of **11** is shown in Figure 4; selected metrical data are listed in Table 1. The

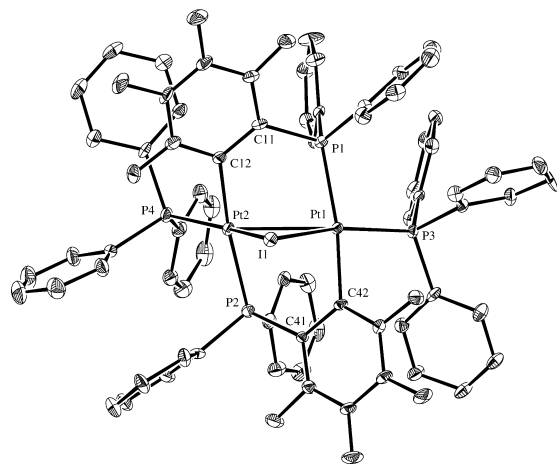


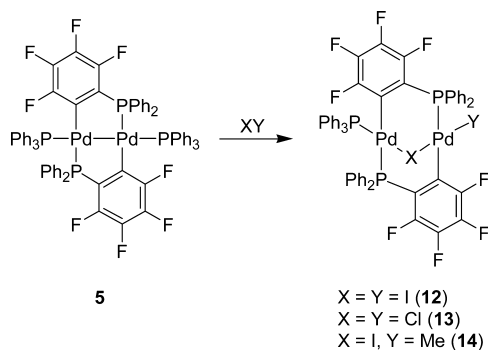
Figure 4. Molecular structure of $[\text{Pt}_2(\mu\text{-I})(\mu\text{-2-C}_6\text{F}_4\text{PPh}_2)_2(\text{PPh}_3)_2]^+$ $[\text{PF}_6]^-$ (**11**) with selected atom labeling. Ellipsoids show 30% probability levels. Hydrogen atoms, PF_6^- counterion, and solvent of crystallization have been omitted for clarity. The crystals of **11** were twinned, arising from a 180° rotation about the (001) reciprocal axis, and the twin elements were refined to 0.815(1):0.185(1).

iodide ligand bridges the two platinum atoms almost symmetrically, with Pt–I distances of 2.7115(7) and 2.7035(7) Å and a narrow Pt–I–Pt angle of 66° . Consistent with indications from the NMR data of a weakening of the Pt–Pt interaction, the Pt...Pt separation of 2.9478(5) Å is significantly greater than that of **9**.

In contrast with the diplatinum(I) complex $[\text{Pt}_2\{\mu\text{-2-C}_6\text{H}_4\text{P}(\text{Ph})\text{CH}_2\text{CH}_2\text{PPh}_2\}_2]$,²⁶ complex **9** did not react with an excess of methyl iodide, probably because the nucleophilicity of the dimetal unit is reduced by the electron-withdrawing fluoro substituents in the bridging group.

2. Dipalladium(I). The complex $[\text{Pd}_2^{\text{I}}(\mu\text{-2-C}_6\text{F}_4\text{PPh}_2)_2(\text{PPh}_3)_2]$ (**5**) reacted immediately with one equivalent of iodine to give a neutral, orange, microcrystalline, iodo-bridged dipalladium(II) complex, $[\text{Pd}_2\text{I}(\mu\text{-I})(\mu\text{-2-C}_6\text{F}_4\text{PPh}_2)_2(\text{PPh}_3)]$ (**12**), which was isolated in ca. 90% yield; the corresponding reaction of **5** with one equivalent of iodobenzene dichloride gave the yellow chloro analogue $[\text{Pd}_2\text{Cl}(\mu\text{-Cl})(\mu\text{-2-C}_6\text{F}_4\text{PPh}_2)_2(\text{PPh}_3)]$ (**13**). There was no evidence in either case for the formation of the dipalladium analogue of the diplatinum(II) cation **11**. Complex **5** also underwent oxidative addition with methyl iodide to give the neutral iodo-bridged complex $[\text{Pd}_2\text{Me}(\mu\text{-I})(\mu\text{-2-C}_6\text{F}_4\text{PPh}_2)_2(\text{PPh}_3)]$ (**14**) containing a terminal methyl group, together with $[\text{Ph}_3\text{MeP}]\text{I}$, which was identified by ^{31}P NMR spectroscopy and mass spectrometry. These reactions are summarized in Scheme 7.

Scheme 7



The ESI mass spectra of **12** and **13** show peaks due to $[\text{M} + \text{Na}]^+$, while that of **14** has peaks assignable to $[\text{M} - \text{I}]^+$ and $[\text{M} - \text{Me}]^+$. The ^{31}P NMR spectrum of **12** shows three, equally intense signals (multiplets, due to P–F coupling), at δ 35.5, due to coordinated PPh_3 , and at δ 7.1 and 4.2, due to the inequivalent ^{31}P nuclei of the bridging 2- $\text{C}_6\text{F}_4\text{PPh}_2$ groups. In the case of **13**, the ^{31}P signals of 2- $\text{C}_6\text{F}_4\text{PPh}_2$ accidentally coincide at δ 4.6 in C_6D_6 , but appear as well-separated multiplets in CD_2Cl_2 (δ 4.4 and 3.3). The corresponding resonances for **14** in C_6D_6 are at δ 29.4 (PPh_3) and at 18.0 and 11.3 (2- $\text{C}_6\text{F}_4\text{PPh}_2$). The ^{19}F NMR spectra of **12**–**14** each contain eight multiplets in the usual region, confirming the inequivalence of the 2- $\text{C}_6\text{F}_4\text{PPh}_2$ groups. In the ^1H NMR spectrum of **14** the Pd–Me resonance appears at δ 1.82 as a doublet of doublets with separations of 2.7 and 7.5 Hz, presumably arising from ^{31}P and ^{19}F coupling. The Raman spectrum of **13** shows a strong $\nu(\text{Pd}\text{--Cl})$ band at 340 cm^{-1} , typical for Cl *trans* to Cl in planar palladium(II) complexes; there are also bands at 287 and 258 cm^{-1} , which can be assigned to the $\nu(\text{Pd}\text{--Cl})$ vibrations of an unsymmetrical Pd–Cl–Pd bridge. The Raman spectrum of **12** contains two strong bands at 136 and 142 cm^{-1} assignable to $\nu(\text{Pd}\text{--I})$, while **14** shows just one such band at 154 cm^{-1} . Similar bands have been observed in the Raman spectra of *trans*- $[\text{PdI}_2(\text{PEt}_3)_2]$ (140 cm^{-1})²⁷ and $[\text{Bu}_4\text{N}]_2[\text{Pd}_2\text{I}_6]$ (143 cm^{-1}).²⁸

The molecular structures of **12–14**, determined by single-crystal X-ray analysis, confirm the conclusions drawn from the spectroscopic data. The structure of **12** is shown in Figure 5,

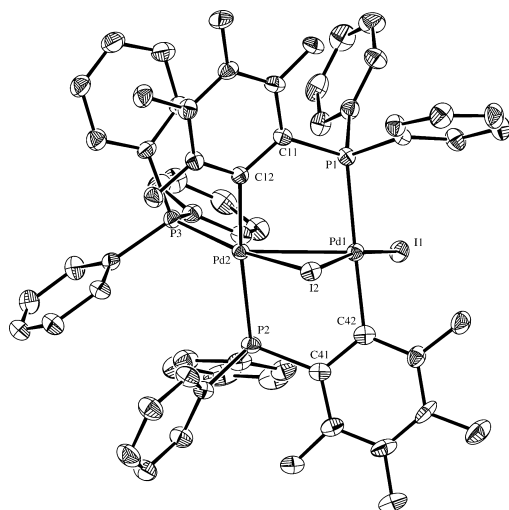


Figure 5. Molecular structure of $[\text{Pd}_2\text{I}(\mu\text{-I})(\mu\text{-}2\text{-C}_6\text{F}_4\text{PPh}_2)_2(\text{PPh}_3)]$ (**12**) with selected atom labeling. Ellipsoids show 30% probability levels. Hydrogen atoms and solvent of crystallization have been omitted for clarity.

and selected metrical data for **12–14** are listed in Table 1. All three compounds have typical A-frame structures with bridging halogen atoms; **12** and **13** also have terminal halogen atoms, while **14** has an η^1 -methyl group in place of the axial PPh_3 of the precursor **5**. As expected, the Pd...Pd separations in **12–14** (ca. 2.81 Å) exceed that in **5** [2.5740(3) Å]. In **12** and **13**, the Pd–halide bridge distance *trans* to the terminal halide [2.6529(7) Å in **12**, 2.3507(6) Å in **13**] is significantly less than that *trans* to PPh_3 [2.7090(6) Å in **12**, 2.4261(6) Å in **13**], consistent with the relative *trans* influences of the halide ions and PPh_3 ; both are greater than the corresponding terminal Pd–halide distances [2.5995(7) Å in **12**, 2.3201(7) Å in **13**]. Similarly, in **14**, the Pd–I (bridge) distance *trans* to Me [2.7386(5) Å] exceeds that *trans* to PPh_3 [2.7101(5) Å], and although the trend is consistent with the relative *trans* influences of I^- and Me^- , the difference is unexpectedly small. Moreover, the observed Pd–C distance in **14** [2.162(4) Å] is significantly outside the range of 2.02–2.09 Å found for Pd–C (Me or Et) bond lengths *trans* to a variety of ligands.²⁹ These observations indicate that partial isomorphous replacement of methyl by iodine may have occurred during crystallization.³⁴

Although complex **5** reacted with iodobenzene, the product, isolated in 58% yield, was not the hoped-for phenyl analogue of **12**, but rather a colorless, monomeric palladium(II) complex, *cis*- $[\text{Pd}(\kappa^2\text{-C},P\text{-}2\text{-C}_6\text{F}_4\text{PPh}_2)(\kappa\text{-C}\text{-}2\text{-C}_6\text{F}_4\text{PPh}_2)(\text{PPh}_3)]$ (**15**) (Scheme 8). The only other product, tentatively identified by ^{31}P NMR spectroscopy, was $[\text{Ph}_4\text{P}]^+$, arising from quaternization of the released Ph_3P by iodobenzene. The ^{31}P NMR spectrum of **15** contains three resonances of equal intensity at δ 19.2, –2.8, and –65.1, each broadened by poorly resolved ^{19}F and ^{31}P coupling; the peaks are assigned to coordinated PPh_3 , noncoordinated PPh_2 , and $\kappa^2\text{-C},P\text{-}2\text{-C}_6\text{F}_4\text{PPh}_2$, respectively. The molecular structure of **15**, which is shown in Figure 6, together with selected bond distances and angles, confirms the conclusions drawn from the spectroscopic data and shows the

Scheme 8

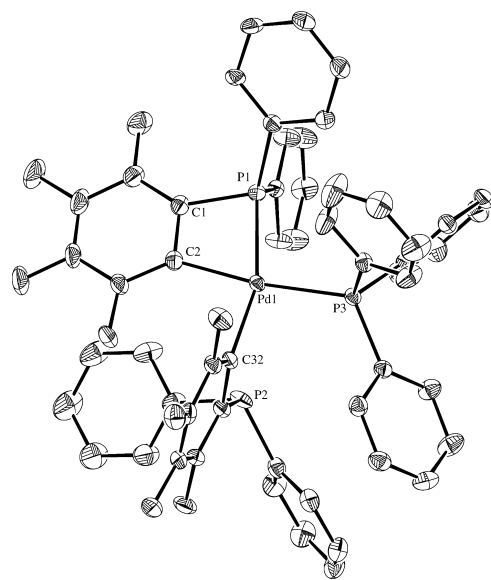
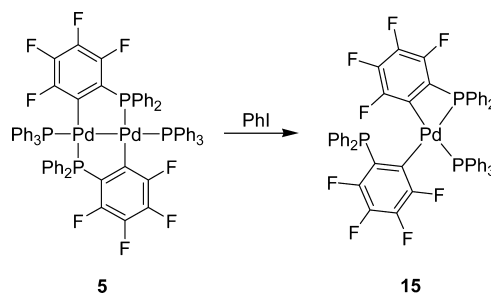


Figure 6. Molecular structure of *cis*- $[\text{Pd}(\kappa^2\text{-C},P\text{-}2\text{-C}_6\text{F}_4\text{PPh}_2)(\kappa\text{-C}\text{-}2\text{-C}_6\text{F}_4\text{PPh}_2)(\text{PPh}_3)]$ (**15**) with selected atom labeling. Ellipsoids show 30% probability levels, and hydrogen atoms have been omitted for clarity. Selected bond distances (Å) and angles (deg): Pd(1)–P(1) 2.3506(6), Pd(1)–P(3) 2.3385(5), Pd(1)–C(2) 2.069(2), Pd(1)–C(32) 2.038(2), P(1)–Pd(1)–C(2) 69.34(6), P(1)–Pd(1)–P(3) 104.722(19), P(3)–Pd(1)–C(32) 93.72(6), C(2)–Pd(1)–C(32) 92.22(8), P(1)–Pd(1)–C(32) 161.55(6), P(3)–Pd(1)–C(2) 172.63(6).

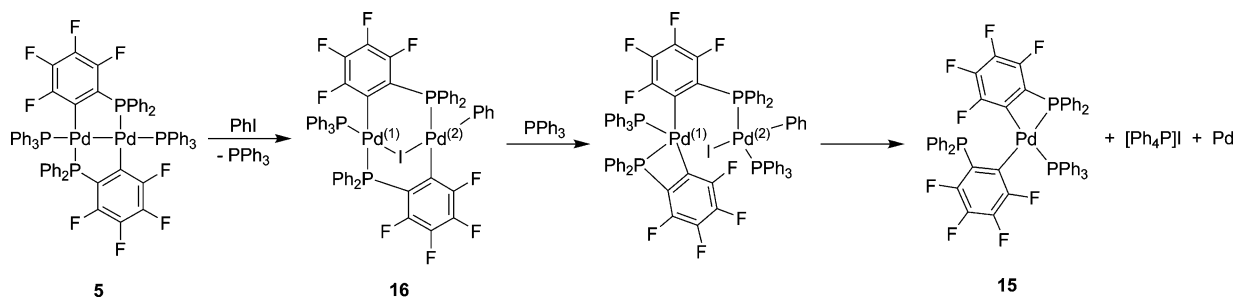
two phosphorus atoms to be mutually *cis*. The bite angle of the chelate group [69.34(6)°] is typical of *ortho*-metalated triarylphosphines.¹

Attempts to generate **15** by heating complex **4** with an excess of PPh_3 were unsuccessful. Evidently the fluorine substituents strengthen the binding of the whole chelate ring, not just the metal–carbon σ -bonds, since $[\text{Pt}(\kappa^2\text{-}2\text{-C}_6\text{H}_4\text{PPh}_2)_2]$ readily undergoes stepwise opening of its chelate rings with tertiary phosphines.³⁵ Complex **15** was shown spectroscopically to be formed when $[\text{Pd}_2\text{Cl}_4(\text{PPh}_3)_2]$ was treated with two equivalents of 2- $\text{LiC}_6\text{F}_4\text{PPh}_2$, but the reaction was not clean and other unidentified products were present.

DISCUSSION

The complexes $[\text{Pd}_2^1(\mu\text{-}2\text{-C}_6\text{F}_4\text{PPh}_2)_2(\text{L})_2]$ [$\text{L} = \text{PPh}_3$ (**5**), AsPh_3 (**6**), $^t\text{BuNC}$ (**7**)] join an extensive class of dipalladium(I) complexes in which one or two ligands, either anionic or neutral, bridge the two $4d^9$ metal centers. Anionic bridging ligands that have been used include halide, η^3 -allyl, η^3 -cyclopentadienyl, dialkyl- or diaryl-phosphido, and alkyl- or aryl-thiolato; neutral ligands include carbon monoxide, arenes,

Scheme 9



dienes, 1,1-bis(diphenylphosphino)methane, $\text{Ph}_2\text{PCH}_2\text{PPh}_2$ (dppm), 1,1-bis(diphenylphosphino)amine, $\text{Ph}_2\text{PNHPPH}_2$ and 2-(diphenylphosphino)pyridine, $(2\text{-C}_5\text{H}_4\text{N})\text{PPh}_2$ 2- Ph_2Ppy .^{36–40} Dipalladium(I) species continue to be of interest because of their possible role in the catalysis of numerous C–C and C–N bond-forming reactions by palladium compounds.⁴¹ An unusual feature of our complexes is the presence of a Pd–C(aryl) bond as part of the bridging ligand. Indeed, the only extensive series of dipalladium(I) complexes containing any metal–aryl carbon σ -bonds, prepared by Usón, Forniés, et al.,¹⁰ are of the types $[\text{Pd}_2(\text{Ar})\text{X}(\mu\text{-dppm})_2]$ (Ar = C_6F_5 , X = Cl, Br, I, NCO, C_6F_5 ; Ar = C_6Cl_5 , X = Cl, C_6F_5) and $[\text{Pd}_2(\text{Ar})\text{X}\{\mu\text{-(Ph}_2\text{P)}_2\text{NH}\}_2]$; like our compounds, they are probably stabilized by the electron-withdrawing substituents in the aryl groups. Stille et al.⁴² have generated and characterized the thermally unstable methyl dipalladium(I) compounds $[\text{Pd}_2(\text{Me})\text{Cl}(\mu\text{-dppm})_2]$ and $[\text{Pd}_2(\text{Me})_2(\mu\text{-dppm})_2]$ at -78°C . So far as we know, the only example of a dipalladium(I) complex in which a Pd–C σ -bond forms part of the bridging ligand is $[\text{Pd}_2(\text{L})_2(\mu\text{-dppm})\{\mu\text{-C,P-Ph}_2\text{PCHP(O)PPh}_2\}]$, where the axial ligand L is 2,6-xylyl isocyanide; it results from the deprotonation and subsequent aerial oxidation of the salt $[\text{Pd}_2(\text{L})_2(\mu\text{-dppm})_2][\text{PF}_6]_2$.⁴³

The method of comproportionation between the palladium(II) precursor 4 and the palladium(0) complexes $[\text{PdL}_4]$ (L = PPh_3 , AsPh_3) to give 5 and 6 follows a strategy that has been widely applied to the synthesis of dipalladium(I) complexes.^{35,38,44} However, in the case of L = $t\text{BuNC}$, attempted comproportionation gives complex 8, in which the 2- $\text{C}_6\text{F}_4\text{PPh}_2$ ligands bridge head-to-head rather than head-to-tail. 8 can be described as a heterovalent Pd(II)–Pd(0), $4d^8\text{--}4d^{10}$, complex in which a lone pair of electrons is donated from Pd(0) to Pd(II), although the electron distribution in the Pd...Pd interaction is unlikely to be as extreme as implied by this description. The Pd...Pd separations in 7 and 8 are not very different. The presence of HT and HH isomers of dipalladium(I) and diplatinum(I) complexes containing unsymmetrical bridging ligands such as $\text{Ph}_2\text{AsCH}_2\text{PPh}_2$,⁴⁵ Ph_2Ppy ,^{46,47} and $\text{Ph}_2\text{PCH}_2\text{SMe}$ ⁴⁸ is well established. Both isomers retain the +1 oxidation state for the metal atoms. Although the HT isomers in these cases appear to be thermodynamically favored, the HT Pd(I)–Pd(I) isomer 7 and the HH Pd(II)–Pd(0) isomer 8 do not interconvert in solution. The factors that control the formation of 8 in the attempted comproportionation, and the question whether HH isomers are intermediates in the comproportionations leading to 5 and 6, remain to be investigated.

The formation of A-frame complexes by oxidative addition of halogens or methyl iodide to complex 5 is clearly analogous to the formation of similar species by the oxidative addition of

small molecules to $[\text{Pd}_2(\mu\text{-dppm})_3]$ ⁴⁷ and $[\text{M}_2\text{X}_2(\mu\text{-dppm})_2]$ (M = Pd, Pt).^{35,36,38,49,50} However, oxidative additions to 5 are accompanied by loss of one of the axial ligands to give neutral adducts, a reaction that does not occur in the addition of halogens to the diplatinum(I) analogues 3a, 3b, and 9. Palladium(II) complexes are, in general, more labile than their platinum(II) counterparts, and the trend obviously continues in the dimetal(I) series. The unexpected formation of $\text{cis-}[\text{Pd}(\kappa^2\text{C,P-2-C}_6\text{F}_4\text{PPh}_2)(\kappa\text{C-2-C}_6\text{F}_4\text{PPh}_2)(\text{PPh}_3)]$ (15) from the reaction of iodobenzene with complex 5 can be accounted for by the sequence shown in Scheme 9. In the first step, iodobenzene adds oxidatively to the Pd–Pd center, with loss of one PPh_3 , to form a μ -iodo(phenyl) species 16 analogous to the methyl complex 14. In the second step, the metal–carbon σ -bond of one of the μ -2- $\text{C}_6\text{F}_4\text{PPh}_2$ ligands migrates to the adjacent metal atom [i.e., from Pd(2) to Pd(1) in Scheme 9], thus generating κ^2 -2- $\text{C}_6\text{F}_4\text{PPh}_2$ on Pd(1) and cleaving the Pd(1)–I bond. At this stage, PPh_3 can reassociate with Pd(2). A similar migration has been invoked as the first step of the rearrangement of the homovalent dihalodigold(II) complexes $[\text{Au}_2\text{X}_2(\mu\text{-2-C}_6\text{F}_4\text{PPh}_2)_2]$ (X = halide) to their heterovalent gold(I)–gold(III) isomers $[\text{XAu}^{\text{I}}(\mu\text{-2-Ph}_2\text{PC}_6\text{F}_4\text{-Au}^{\text{III}}\text{X}(\kappa^2\text{C,P-2-C}_6\text{F}_4\text{PPh}_2))]$.⁵¹ The sequence is completed by cleavage of the Pd(2)–P bond from the remaining μ -2- $\text{C}_6\text{F}_4\text{PPh}_2$ ligand, giving 15, and elimination of $[\text{Ph}_4\text{P}]\text{I}$ from Pd(2). Since the formation of metallic palladium is not observed, the fate of Pd(2) is unclear; however, in general agreement with the proposed course of the reaction, it has been reported that $[\text{PdI}(\text{Ph})(\text{PPh}_3)_2]$ eliminates $[\text{Ph}_4\text{P}]\text{I}$ on heating⁵² and that the quaternization of PPh_3 by aryl bromides is catalyzed by $[\text{Pd}(\text{OAc})_2]$ in DMF,⁵³ a reaction that probably involves Pd(0).

Finally, we note that the work reported here extends the series of dinuclear palladium complexes containing bridging 2- $\text{C}_6\text{F}_4\text{PPh}_2$ ligands so that it now spans the oxidation states Pd(I)–Pd(I) ($4d^9\text{--}4d^9$) (R = F), Pd(II)–Pd(II) ($4d^8\text{--}4d^8$) (R = H, F),^{7–9} and Pd(III)–Pd(III) ($4d^7\text{--}4d^7$) (R = H).⁵⁴

EXPERIMENTAL SECTION

General Comments. Toluene, diethyl ether, dichloromethane, and *n*-hexane were dried by the use of a standard column drying system. The complexes $[\text{M}(\kappa^2\text{-2-C}_6\text{F}_4\text{PPh}_2)_2]$ (M = Pt, Pd),⁹ $[\text{Pt}(\text{PPh}_3)_3]$,⁵⁵ $[\text{Pd}(\text{PPh}_3)_4]$,⁵⁶ $[\text{Pd}(\text{AsPh}_3)_4]$,⁵⁷ and $[\text{Pd}(\eta^5\text{-Cp})(\eta^3\text{-allyl})]$ ⁵⁸ were prepared by literature methods. $[\text{Pt}_3(\text{CN}^t\text{Bu})_6]$ was prepared by a reported method⁵⁹ using $[\text{Pt}(\text{norbornene})_3]$ ^{60,61} instead of $[\text{Pt}(1,5\text{-cyclooctadiene})_2]$; all other reagents were commercially available and used as received. ^1H (300 MHz), ^{19}F (282 MHz), and ^{31}P (121 MHz) NMR spectra were measured as C_6D_6 solutions, unless otherwise stated, on a Bruker Avance 300 spectrometer at room temperature. NMR spectral simulations were made by use of the gNMR program.⁶² Raman spectra were obtained on a Perkin-Elmer

Table 2. Crystal and Refinement Data for [Pd₂^I(μ-2-C₆F₄PPh₂)₂(L)₂] [L = PPh₃ (5), AsPh₃ (6), ^tBuNC (7)], [Pd₂^{0/II}(μ-2-C₆F₄PPh₂)₂(CN^tBu)₂] (8), [Pt₂^I(μ-2-C₆F₄PPh₂)₂(L)₂] [L = PPh₃ (9), ^tBuNC (10)], [Pt₂(μ-I)(μ-2-C₆F₄PPh₂)₂(PPh₃)₂][PF₆] (11), [Pd₂^I(μ-I)(μ-2-C₆F₄PPh₂)₂(PPh₃)] (12), [Pd₂Cl(μ-Cl)(μ-2-C₆F₄PPh₂)₂(PPh₃)] (13), [Pd₂Me(μ-I)(μ-2-C₆F₄PPh₂)₂(PPh₃)] (14), and [Pd(κ²-C,*P*-2-C₆F₄PPh₂)(κC-2-C₆F₄PPh₂)(PPh₃)] (15)

	5	6	7	8
formula	C ₇₂ H ₅₀ F ₈ P ₄ Pd ₂	C ₇₂ H ₅₀ As ₂ F ₈ P ₂ Pd ₂	C ₄₆ H ₃₈ F ₈ N ₂ P ₂ Pd ₂ ·3C ₆ H ₆	C ₄₆ H ₃₈ F ₈ N ₂ P ₂ Pd ₂
fw	1403.87	1491.76	1279.89	1045.55
cryst syst	monoclinic	monoclinic	orthorhombic	tetragonal
space group	<i>P</i> 2 ₁ / <i>n</i>	<i>P</i> 2 ₁ / <i>n</i>	<i>Pbcn</i>	<i>P</i> 4 ₁ 2 ₁ 2
cryst color, habit	brown, needle	orange, block	yellow, needle	pale yellow, block
<i>a</i> (Å)	12.9954(1)	13.1071(2)	19.7128(3)	12.2048(2)
<i>b</i> (Å)	22.8850(2)	23.2833(2)	21.4914(3)	12.2048(2)
<i>c</i> (Å)	20.2845(2)	20.0903(3)	13.9542(2)	30.1528(4)
α (deg)				
β (deg)	93.0380(6)	93.2236(6)		
γ (deg)				
<i>V</i> (Å ³)	6024.13(9)	6121.39(14)	5911.78(15)	4491.47(12)
<i>Z</i>	4	4	4	4
<i>D</i> _{calc} (g cm ⁻³)	1.548	1.619	1.438	1.546
cryst dimens	0.40 × 0.09 × 0.05	0.16 × 0.07 × 0.05	0.28 × 0.08 × 0.07	0.35 × 0.30 × 0.30
μ (mm ⁻¹)	0.77	1.78	0.73	0.94
no. indep reflns (<i>R</i> _{int})	13794 (0.060)	14113 (0.097)	6771 (0.064)	6518 (0.039)
no. obsd reflns	9166 [<i>I</i> > 2σ(<i>I</i>)]	9981 [<i>I</i> > 2σ(<i>I</i>)]	4207 [<i>I</i> > 2σ(<i>I</i>)]	5518 [<i>I</i> > 2σ(<i>I</i>)]
no. params refined	775	775	380	327
<i>R</i>	0.026	0.042	0.027	0.020
<i>R</i> _w	0.075	0.076	0.128	0.054
GOF	0.96	0.96	0.94	0.91
ρ_{\max}/ρ_{\min} (e Å ⁻³)	0.71/−0.82	1.30/−1.23	0.65/−0.85	0.45/−0.42
	9	10	11	12
formula	C ₇₂ H ₅₀ F ₈ P ₄ Pt ₂	C ₄₆ H ₃₈ N ₂ F ₈ P ₂ Pt ₂	C ₇₂ H ₅₀ F ₈ IP ₄ Pt ₂ PF ₆ ·2CH ₂ Cl ₂	2(C ₃₄ H ₃₅ F ₈ I ₂ P ₃ Pd ₂)·C ₅ H ₁₂ ·C ₆ H ₆
fw	1581.25	1222.90	2022.98	2941.04
cryst syst	monoclinic	monoclinic	triclinic	orthorhombic
space group	<i>P</i> 2 ₁ / <i>n</i>	<i>P</i> 2 ₁ / <i>c</i>	<i>P</i> $\bar{1}$	<i>P</i> 2 ₁ 2 ₁
cryst color, habit	yellow, needle	colorless, needle	yellow, plate	orange, plate
<i>a</i> (Å)	12.9761(1)	15.1933(7)	12.8010(2)	11.3916(2)
<i>b</i> (Å)	22.8436(2)	16.7722(8)	14.8766(3)	21.7240(4)
<i>c</i> (Å)	20.3033(1)	17.8033(8)	20.1361(4)	44.4879(8)
α (deg)			106.5093(10)	
β (deg)	92.9339(4)	109.5320(10)	93.0296(12)	
γ (deg)			105.5032(10)	
<i>V</i> (Å ³)	6010.42(8)	4275.7(3)	3508.17(12)	11009.5(3)
<i>Z</i>	4	4	2	4
<i>D</i> _{calc} (g cm ⁻³)	1.747	1.900	1.915	1.774
cryst dimens	0.42 × 0.14 × 0.12	0.20 × 0.06 × 0.06	0.29 × 0.22 × 0.02	0.42 × 0.08 × 0.08
μ (mm ⁻¹)	4.83	6.68	4.77	1.93
no. indep reflns (<i>R</i> _{int})	17572 (0.051)	93407 (0.079)	16027 (0.076)	19318 (0.048)
no. obsd reflns	14 066 [<i>I</i> > 2σ(<i>I</i>)]	18 795 [<i>I</i> > 2σ(<i>I</i>)]	13 226 [<i>I</i> > 2σ(<i>I</i>)]	16 087 [<i>I</i> > 2σ(<i>I</i>)]
no. params refined	775	547	902	1297
<i>R</i>	0.023	0.038	0.058	0.029
<i>R</i> _w	0.062	0.069	0.112	0.094
GOF	0.77	0.97	0.98	0.77
ρ_{\max}/ρ_{\min} (e Å ⁻³)	2.09/−1.38	1.55/−1.43	2.18/−1.82	0.83/−0.77
	13	14	15	
formula	C ₅₄ H ₃₅ Cl ₂ F ₈ P ₃ Pd ₂	C ₅₅ H ₃₈ F ₈ IP ₃ Pd ₂ ·C ₆ H ₆	C ₅₄ H ₃₅ F ₈ P ₃ Pd	
fw	1212.43	1361.63	1035.18	
cryst syst	orthorhombic	monoclinic	monoclinic	
space group	<i>Pca</i> 2 ₁	<i>P</i> 2 ₁ / <i>a</i>	<i>P</i> 2 ₁ / <i>a</i>	
cryst color, habit	colorless, block	orange, plate	colorless, plate	
<i>a</i> (Å)	17.0645(6)	18.0043(4)	11.3738(1)	
<i>b</i> (Å)	16.4054(6)	17.8269(5)	12.0304(1)	
<i>c</i> (Å)	16.9043(6)	18.8760(5)	12.0304(1)	
α (deg)				

Table 2. continued

	13	14	15
β (deg)		94.7219(17)	98.3916(5)
γ (deg)			
V (Å ³)	4732.4(3)	6037.9(3)	4443.46(7)
Z	4	4	4
D_{calc} (g cm ⁻³)	1.702	1.498	1.547
cryst dimens	0.08 × 0.06 × 0.04	0.30 × 0.24 × 0.07	0.26 × 0.14 × 0.05
μ (mm ⁻¹)	1.05	1.25	0.60
no. indep reflns (R_{int})	56899 (0.037)	13915 (0.090)	10183 (0.054)
no. obsd reflns	15617 [$I > 2\sigma(I)$]	7677 [$I > 2\sigma(I)$]	8133 [$I > 2\sigma(I)$]
no. params refined	622	676	760
R	0.031	0.044	0.031
R_w	0.064	0.112	0.069
GOF	1.017	0.83	0.97
$\rho_{\text{max}}/\rho_{\text{min}}$ (e Å ⁻³)	0.75/−0.39	2.03/−1.99	0.59/−0.55

Raman Station 400F spectrometer as solids in open glass capillaries, and infrared spectra on a Perkin-Elmer Spectrum 2000 FT spectrometer as KBr discs or Nujol mulls. Electro spray mass spectra were measured on an HP 5970 MSD spectrometer, and elemental analyses were carried out by the Microanalytical Unit at the Research School of Chemistry, ANU.

X-ray Crystallography. Crystals of **5**, **9**, **12**, **14**, and **15** suitable for X-ray crystallography were obtained from benzene/pentane, **6** and **7** from benzene/hexane, **8**, **11**, and **13** from dichloromethane/methanol, and **10** from benzene. The crystals were coated in viscous oil and mounted on fine-drawn capillaries. Crystal data and details of data collection are given in Table 2. Data for complexes **10** and **13** were collected at 150 K on a D8 Bruker diffractometer equipped with an APEX2 area detector using graphite-monochromated Mo $K\alpha$ radiation ($\lambda = 0.71073$ Å) from a 1 μS microsource. Geometric and intensity data were collected using SMART software.⁶³ The data were processed using SAINT,⁶⁴ and corrections for absorption were applied using SADABS.⁶⁵ The structures were solved by direct methods and refined with full-matrix least-squares methods on F^2 using the SHELXL-TL package.⁶⁶ Data for the remaining complexes were collected at 200 K on a Nonius-Kappa CCD diffractometer using graphite-monochromated Mo $K\alpha$ radiation ($\lambda = 0.71073$ Å). Data were measured by use of COLLECT.⁶⁷ The intensities of reflections were extracted, and the data were reduced by use of the computer programs Denzo and Scalepack.⁶⁸ The crystal structures were solved by direct methods⁶⁹ and refined by use of the program CRYSTALS.⁷⁰ Neutral atom scattering factors,⁷¹ the values of $\Delta f'$ and $\Delta f''$, and mass attenuation coefficients⁷² were taken from standard compilations.

Preparations. $[\text{Pd}_2(\mu\text{-}2\text{-C}_6\text{F}_4\text{PPh}_2)_2(\text{PPh}_3)_2]$ (**5**). (a) To a mixture of *trans*- $[\text{Pd}(\kappa^2\text{-}2\text{-C}_6\text{F}_4\text{PPh}_2)_2]$ (200 mg, 0.26 mmol) and $[\text{Pd}(\text{PPh}_3)_4]$ (299 mg, 0.26 mmol) was added toluene (20 mL) under an argon atmosphere, and the orange-red solution was stirred at room temperature overnight. The solution was filtered through Celite, and the filtrate was evaporated to dryness. The orange-red residue was dissolved in CH_2Cl_2 , MeOH was added, and the volume of the solution was reduced *in vacuo*. The resulting orange precipitate was isolated by filtration, washed with MeOH, and dried *in vacuo* (320 mg, 83%). ¹H NMR: δ 6.4–8.2 (m, 50H, aromatic). ³¹P NMR: δ 8.4 (s), −19.3 (br s). ¹⁹F NMR: δ −105.1 (m), −128.9 (m), −153.1 (m), −162.9 (m). Raman (cm^{-1}): 135, $\nu(\text{Pd-Pd})$. ESI-MS (m/z): 1404 $[\text{M}]^+$. Anal. Calcd for $\text{C}_{72}\text{H}_{50}\text{F}_8\text{P}_4\text{Pd}_2$: C 61.60; H 3.59; F 10.83. Found: C 61.51; H 3.53; F 10.40.

(b) To a solution of *trans*- $[\text{Pd}(\kappa^2\text{-}2\text{-C}_6\text{F}_4\text{PPh}_2)_2]$ (225 mg, 0.29 mmol) in toluene (20 mL) was added PPh_3 (153 mg, 0.58 mmol) under argon. The colorless solution was cooled to -78 °C, and solid $[\text{Pd}(\eta^5\text{-Cp})(\eta^3\text{-allyl})]$ (62 mg, 0.29 mmol) was added. The mixture was stirred at -78 °C for several hours, then allowed to warm to room temperature overnight. The dark orange-brown solution was evaporated to dryness, and the residue was dissolved in CH_2Cl_2 and filtered through Celite. MeOH was added to the filtrate, and the

solution was evaporated. The resulting orange precipitate was isolated by filtration, washed with MeOH, and dried *in vacuo* (320 mg, 78%). Spectral data were identical to those of (a) above.

$[\text{Pd}_2(\mu\text{-}2\text{-C}_6\text{F}_4\text{PPh}_2)_2(\text{AsPh}_3)_2]$ (**6**). To a mixture of *trans*- $[\text{Pd}(\kappa^2\text{-}2\text{-C}_6\text{F}_4\text{PPh}_2)_2]$ (200 mg, 0.26 mmol) and $[\text{Pd}(\text{AsPh}_3)_4]$ (344 mg, 0.26 mmol) was added toluene (40 mL) under an argon atmosphere, and the yellow suspension was heated to 60 °C for 2 h. The solution was allowed to cool and filtered through Celite, and the solvent was removed *in vacuo*. The orange residue was dissolved in CH_2Cl_2 , MeOH was added, and the volume of the solution was reduced. The yellow precipitate was isolated, washed with MeOH, and dried *in vacuo* (370 mg, 96%). ¹H NMR: δ 6.4–8.2 (m, 50H, aromatic). ³¹P NMR: δ −17.6 (br s). ¹⁹F NMR: δ −105.5 (m), −129.8 (m), −153.2 (m), −162.6 (m). Raman (cm^{-1}): 131, $\nu(\text{Pd-Pd})$. ESI-MS (m/z): 1492 $[\text{M}]^+$. Anal. Calcd for $\text{C}_{72}\text{H}_{50}\text{As}_2\text{F}_8\text{P}_2\text{Pd}_2$: C 57.97; H 3.38; F 10.19. Found: C 57.95; H 3.55; F 10.24.

$[\text{Pd}_2(\mu\text{-}2\text{-C}_6\text{F}_4\text{PPh}_2)_2(\text{CN}^i\text{Bu})_2]$ (**7**). To a solution of **6** (100 mg, 0.07 mmol) in CH_2Cl_2 (4 mL) was added ^tBuNC (17 μL , 0.14 mmol). The color immediately faded from orange to yellow, and after the solution had been stirred for 10 min, hexane was added. The volume of the solution was reduced *in vacuo*, causing a yellow solid to precipitate. This was isolated by filtration, washed with hexane, and dried *in vacuo* (64 mg, 91%). ¹H NMR: δ 0.56 (s, 18H, ^tBu), 6.8–7.9 (m, 20H, aromatic). ³¹P NMR: δ −14.3 (br s). ¹⁹F NMR: δ −109.1 (m), −130.2 (m), −155.4 (m), −162.2 (m). IR (KBr, cm^{-1}): 2164, $\nu(\text{N}\equiv\text{C})$. Raman (cm^{-1}): 129, $\nu(\text{Pd-Pd})$. ESI-MS (m/z): 1046 $[\text{M}]^+$, 1063 $[\text{M} + \text{O} + \text{H}]^+$. Anal. Calcd for $\text{C}_{46}\text{H}_{38}\text{F}_8\text{N}_2\text{P}_2\text{Pd}_2$: C 52.84; H 3.66; N 2.68; F 14.54. Found: C 52.72; H 4.00; N 2.79; F 14.50.

$[\text{Pd}_2(\mu\text{-}2\text{-C}_6\text{F}_4\text{PPh}_2)_2(\text{CN}^i\text{Bu})_2]$ (**8**). To a solution of *trans*- $[\text{Pd}(\kappa^2\text{-}2\text{-C}_6\text{F}_4\text{PPh}_2)_2]$ (200 mg, 0.26 mmol) in toluene (20 mL) was added ^tBuNC (60 μL , 0.53 mmol) under argon. The colorless solution was cooled to -78 °C, and $[\text{Pd}(\eta^5\text{-Cp})(\eta^3\text{-allyl})]$ (55 mg, 0.26 mmol) was added. The mixture was stirred at -78 °C for several hours, then allowed to warm to room temperature overnight. The solvent was removed *in vacuo*, and the residue was dissolved in CH_2Cl_2 . After the solution had been filtered through Celite, MeOH was added to the filtrate and the volume of the solution was reduced *in vacuo*. The pale yellow solid that precipitated was isolated, washed with MeOH, and dried *in vacuo* (195 mg, 72%). ¹H NMR: δ 0.45 (s, 9H, ^tBu), 0.63 (s, 9H, ^tBu), 6.9–7.1 (m, 6H, aromatic), 7.2–7.3 (m, 6H, aromatic), 7.5–7.6 (m, 4H, aromatic), 8.3–8.4 (m, 4H, aromatic). ³¹P NMR: δ −13.6 (br s). ¹⁹F NMR: δ −113.5 (m), −130.9 (m), −156.2 (m), −162.7 (m). IR (cm^{-1}): 2159, 2187 (Nujol); 2161, 2188 (KBr), $\nu(\text{N}\equiv\text{C})$. Raman (cm^{-1}): 128, $\nu(\text{Pd-Pd})$. ESI-MS (m/z): 1046 $[\text{M}]^+$, 1079 $[\text{M} + 2\text{O} + \text{H}]^+$. Anal. Calcd for $\text{C}_{46}\text{H}_{38}\text{F}_8\text{N}_2\text{P}_2\text{Pd}_2$: C 52.84; H 3.66; N 2.68; F 14.54. Found: C 52.68; H 3.68; N 2.59; F 14.26.

$[\text{Pt}_2(\mu\text{-}2\text{-C}_6\text{F}_4\text{PPh}_2)_2(\text{PPh}_3)_2]$ (**9**). A mixture of $[\text{Pt}(\kappa^2\text{-}2\text{-C}_6\text{F}_4\text{PPh}_2)_2]$ (140 mg, 0.16 mmol) and $[\text{Pt}(\text{PPh}_3)_3]$ (150 mg, 0.16 mmol) was suspended in toluene (10 mL) under an argon atmosphere, and the yellow mixture was refluxed overnight. After being cooled to room

temperature, the solution was evaporated and EtOH was added. The resulting orange solid was isolated and dissolved in CH₂Cl₂, and MeOH was added. The solution was again evaporated *in vacuo* to give a yellow solid, which was washed with MeOH and dried *in vacuo* (110 mg, 44%). ¹H NMR: δ 0.38 (s, 2H, H₂O), 6.0–8.0 (m, 50H, aromatics). ³¹P NMR: δ –8.2 (P_A, m), 24.4 (P_B, m, J_{AA} 0 Hz, J_{AB} 15 Hz, J_{AB} 15 Hz, J_{AX} 2369 Hz, J_{AX} 133 Hz, J_{BB} 208 Hz, J_{BX} 2001 Hz, J_{BX} 904 Hz). ¹⁹F NMR: δ –105.1 (m, J_{PF} 267 Hz), –129.0 (m), –153.4 (m), –163.0 (m). Raman (cm⁻¹): 126, ν(Pt–Pt). ESI-MS (*m/z*): 1581 [M + H]⁺. Anal. Calcd for C₇₂H₅₀F₈P₄Pt₂·2H₂O: C 53.47; H 3.37; P 7.66. Found: C 53.21; H 3.34; P 7.86.

[Pt₂(μ-2-C₆F₄PPh₂)₂(CN^tBu)₂] (10). A mixture of [Pt(κ²-C₆F₄PPh₂)₂] (105 mg, 0.12 mmol) and [Pt₃(CN^tBu)₆] (44 mg, 0.04 mmol) was dissolved in toluene (20 mL) under an argon atmosphere, and the orange solution was stirred at room temperature overnight. The resulting pale yellow solution was evaporated to dryness, and the residue was recrystallized from CH₂Cl₂/MeOH. The pale yellow solid that precipitated was isolated and dried *in vacuo* (143 mg, 96%). ¹H NMR: δ 0.54 (s, 18H, Bu), 6.8–8.0 (m, 20H, aromatics). ³¹P NMR: δ –7.4 (br s, J_{AX} 2330 Hz, J_{AX} 156, J_{XX} ~2360 Hz). ¹⁹F NMR: δ –109.7 (m, J_{PF} 262 Hz), –130.1 (m), –154.9 (m, J_{PF} 109 Hz), –161.6 (m). ESI-MS (*m/z*): 1223 [M + H]⁺. Anal. Calcd for C₄₆H₃₈N₂F₈P₂Pt₂: C 45.18; H 3.13; N 2.29, F 12.43. Found: C 45.08; H 3.15; N 2.22; F 12.30.

[Pt₂(μ-1)(μ-2-C₆F₄PPh₂)₂(PPh₃)₂]PF₆ (11). To a solution of 9 (110 mg, 0.07 mmol) in CH₂Cl₂ (5 mL) was added I₂ (18 mg, 0.07 mmol) in CH₂Cl₂ (5 mL). After stirring for 10 min, KPF₆ (100 mg, 0.54 mmol) in acetone (10 mL) was added, and the solution was evaporated to dryness. The residue was taken up in CH₂Cl₂ and filtered through Celite, and the filtrate treated with a solution of KPF₆ (100 mg, 0.54 mmol) in acetone (10 mL). The mixture was again evaporated to dryness, taken up in CH₂Cl₂, and filtered through Celite. Hexane was added to the filtrate, and the volume of the solution was reduced *in vacuo*. The yellow solid that precipitated was isolated, washed with hexane, and dried *in vacuo* (120 mg, 93%). ¹H NMR (CD₂Cl₂): δ 6.7–8.0 (m, 50H, aromatic). ³¹P NMR (CD₂Cl₂): δ 10.3 (br s, J_{PF} 128, 4645 Hz), 4.4 (br s, J_{PF} 1972 Hz), –144.5 (sept, J_{PF} 710 Hz). ¹⁹F NMR (CD₂Cl₂): δ –73.6 (d, J_{PF} 710 Hz), –102.8 (m, J_{PF} 195 Hz), –120.2 (m), –150.7 (m), –159.3 (m). Raman (cm⁻¹): 154, ν(Pt–I). ESI-MS (*m/z*): 1707 [M – PF₆]⁺. Anal. Calcd for C₇₂H₅₀F₁₄I₂P₃Pt₂: C 46.67; H 2.72; F 14.35; I 6.85. Found: C 47.18; H 3.01; F 14.79; I 6.77.

[Pd₂(μ-1)(μ-2-C₆F₄PPh₂)₂(PPh₃)] (12). To an orange solution of 5 (100 mg, 0.07 mmol) in CH₂Cl₂ (5 mL) was added a solution of I₂ (18 mg, 0.07 mmol) in CH₂Cl₂ (5 mL). The mixture was stirred for 10 min and evaporated to dryness *in vacuo*. The residue was dissolved in toluene, and the solution was passed down a short silica column. The eluent was evaporated to dryness, and the residue, suspended in Et₂O (10 mL), was stirred rapidly for 1 h. The orange solid was filtered off, washed with Et₂O, and dried *in vacuo* (90 mg, 91%). ¹H NMR: δ 1.12 (t, J 6.9 Hz, 6H, CH₃), 3.26 (q, J 6.9 Hz, 4H, CH₂), 6.2–6.4 (m, 4H, aromatic), 6.6–6.8 (m, 10H, aromatic), 6.9–7.1 (m, 11H, aromatic), 7.5–8.0 (m, 8H, aromatic), 8.3–8.4 (m, 2H, aromatic). ³¹P NMR: δ 33.5 (apparent td, J 6.0, 6.0, 27.2 Hz), 7.1 (m), 4.2 (m). ¹⁹F NMR: δ –102.2 (m), –107.1 (m), –120.6 (m), –123.5 (m), –148.5 (m), –152.1 (m), –159.9 (m), –160.0 (m). Raman (cm⁻¹): 136, 142, ν(Pd–I). ESI-MS (*m/z*): 1419 [M + Na]⁺. Anal. Calcd for C₅₄H₃₅F₈I₂P₃Pd₂·0.7Et₂O: C 47.14; H 2.92; F 10.50; I 17.54. Found: C 47.17; H 2.96; F 10.55; I 17.34.

[Pd₂Cl(μ-Cl)(μ-2-C₆F₄PPh₂)₂(PPh₃)] (13). This complex was made analogously to 12 above by treatment of 5 (109 mg, 0.07 mmol) in CH₂Cl₂ (5 mL) with PhICl₂ (20 mg, 0.07 mmol) in CH₂Cl₂ (5 mL). The product was a yellow solid (75 mg, 76%). ¹H NMR: δ 1.10 (t, J 7.0 Hz, 6H, CH₃), 3.25 (q, J 7.0 Hz, 4H, CH₂), 6.2–7.2 (m, 25H, aromatic), 7.6–8.5 (m, 10H, aromatic). ³¹P NMR: δ 33.3 (apparent ddd, J 2.0, 15.2, 27.5 Hz), 4.6 (m). ¹⁹F NMR: δ –107.8 (m), –112.2 (m), –120.5 (m), –123.8 (m), –149.4 (m), –150.6 (m), –159.0 (m), –160.1 (m). ¹H NMR (CD₂Cl₂): δ 1.19 (t, J 7.0 Hz, 6H, CH₃), 3.47 (q, J 7.0 Hz, 4H, CH₂), 6.1–8.3 (m, 35H, aromatic). ³¹P NMR (CD₂Cl₂): δ 33.5 (apparent dddd, J 2.9, 7.6, 22.3, 26.1 Hz), 4.4 (m),

3.3 (m). ¹⁹F NMR (CD₂Cl₂): δ –107.7 (m), –114.2 (m), –121.5 (m), –123.0 (m), –150.2 (m), –152.0 (m), –159.6 (m), –160.9 (m). Raman (cm⁻¹): 287, 340, ν(Pd–Cl). ESI-MS (*m/z*): 1235 [M + Na]⁺. Anal. Calcd for C₅₄H₃₅Cl₂F₈P₃Pd₂·0.7Et₂O: C 53.96; H 3.35; Cl 5.61; F 12.02. Found: C 54.21; H 3.41; Cl 5.62; F 12.17.

[Pd₂Me(μ-1)(μ-2-C₆F₄PPh₂)₂(PPh₃)] (14). To an orange solution of 5 (100 mg, 0.07 mmol) in CH₂Cl₂ (5 mL) was added MeI (1 mL), and the mixture was stirred at room temperature overnight. After evaporation of the orange solution to dryness, the residue was suspended in toluene, and the mixture was passed down a short silica column. The eluent was evaporated to dryness, and the residue was recrystallized from CH₂Cl₂/hexane to give a golden-orange solid (70 mg, 81%). ¹H NMR: δ 1.82 (dd, J 2.7, 7.5 Hz, 3H, CH₃), 6.3–7.2 (m, 25H, aromatic), 7.5–8.1 (m, 8H, aromatic), 8.3–8.4 (m, 2H, aromatic). ³¹P NMR: δ 29.4 (tm, J 26.5 Hz), 18.0 (m), 11.3 (m). ¹⁹F NMR: δ –106.4 (m), –107.6 (m), –121.6 (m), –122.2 (m), –149.0 (m), –151.7 (m), –161.0 (m), –161.8 (m). Raman (cm⁻¹): 154, ν(Pd–I). ESI-MS (*m/z*): 1156 [M – I]⁺, 1268 [M – Me]⁺. Anal. Calcd for C₅₅H₃₈F₈IP₃Pd₂: C 51.47; H 2.98; F 11.84; I 9.89. Found: C 51.25; H 3.23; F 11.54; I 10.04. A portion of the toluene-insoluble material was carefully removed from the top of the column. The spectroscopic properties of the solid residue were consistent with the presence of [Ph₃MeP]I. ³¹P NMR (CH₂Cl₂/C₆D₆): δ 21.9 [cf. δ 22.2 (CDCl₃)⁷³]. ESI-MS (*m/z*): 277 [M – I]⁺.

cis-[Pd(κ²-C, P-2-C₆F₄PPh₂)(κC-2-C₆F₄PPh₂)(PPh₃)] (15). To an orange solution of 5 (150 mg, 0.11 mmol) in CH₂Cl₂ (10 mL) was added PhI (1 mL), and the mixture was stirred at room temperature in the dark for 6 h. The yellow solution was evaporated to dryness, and the residue, after trituration with MeCN (3 × 5 mL), gave a colorless solid. This was dissolved in CH₂Cl₂, MeCN was added, and the solution was evaporated. The colorless solid that precipitated was isolated by filtration, washed with MeCN, and dried *in vacuo* (64 mg, 58%). ¹H NMR: δ 6.6 (t, J 1.1 Hz, 2H, aromatic), 7.0–7.5 (m, 33H, aromatic). ³¹P NMR: δ 19.2 (br d, J ~13 Hz), –2.8 (br t, J ~21 Hz), –65.1 (m). ¹⁹F NMR: δ –114.4 (m), –125.3 (m), –126.0 (m), –135.6 (m), –150.6 (m), –156.4 (m), –160.4 (m), –162.4 (m). ESI-MS (*m/z*): 1035 [M + H]⁺. Anal. Calcd for C₅₄H₃₅F₈P₃Pd: C 62.65; H 3.41; F 14.68. Found: C 62.70; H 3.53; F 14.72. The ³¹P NMR spectrum of an aliquot of the crude reaction mixture before workup (CH₂Cl₂/C₆D₆) showed the expected resonances due to 15, together with a peak at δ –71.2 and several peaks in the range δ 20–27; an intense singlet resonance at δ 23.4 was consistent with the formation of [Ph₄P]I [cf. δ 23.5 (CDCl₃)⁷³].

■ ASSOCIATED CONTENT

Supporting Information

X-ray crystallographic data in CIF format for complexes 5–15. This material is available free of charge via the Internet at <http://pubs.acs.org>.

■ AUTHOR INFORMATION

Corresponding Author

*E-mail: bennett@rsc.anu.edu.au (M.A.B.); suresh.bhargava@rmit.edu.au (S.K.B.).

Notes

The authors declare no competing financial interest.

■ REFERENCES

- (1) Mohr, F.; Privér, S. H.; Bhargava, S. K.; Bennett, M. A. *Coord. Chem. Rev.* **2006**, *250*, 1851.
- (2) Chakravarty, A. R.; Cotton, F. A.; Tocher, D. A.; Tocher, J. H. *Organometallics* **1985**, *4*, 8.
- (3) Bennett, M. A.; Dirnberger, T.; Hockless, D. C. R.; Wenger, E.; Willis, A. C. *J. Chem. Soc., Dalton Trans.* **1998**, 2367.
- (4) Bender, R.; Bouaoud, S. E.; Braunstein, P.; Dusaosoy, Y.; Merabet, J.; Raya, J.; Rouag, D. *J. Chem. Soc., Dalton Trans.* **1999**, 735.

- (5) Bennett, M. A.; Berry, D. E.; Bhargava, S. K.; Ditzel, E. J.; Robertson, G. B.; Willis, A. C. *J. Chem. Soc., Chem. Commun.* **1987**, 1613.
- (6) Bennett, M. A.; Bhargava, S. K.; Messelhäuser, J.; Privér, S. H.; Welling, L. L.; Willis, A. C. *Dalton Trans.* **2007**, 3158.
- (7) Aarif, A. M.; Estevan, F.; García-Barnabé, A.; Lahuerta, P.; Sanaú, M.; Ubeda, M. A. *Inorg. Chem.* **1997**, 36, 6472.
- (8) Estevan, F.; García-Barnabé, A.; Lahuerta, P.; Sanaú, M.; Ubeda, M. A.; Ramírez de Arellano, M. C. *Inorg. Chem.* **2000**, 39, 5964.
- (9) Bennett, M. A.; Bhargava, S. K.; Keniry, M. A.; Privér, S. H.; Simmonds, P. A.; Wagler, J. A.; Willis, A. C. *Organometallics* **2008**, 27, 5361.
- (10) Usón, R.; Forniés, J. *Adv. Organomet. Chem.* **1988**, 28, 219.
- (11) Alves, O. L.; Vitorge, M.; Sourisseau, C. *Nouv. J. Chim.* **1983**, 7, 231.
- (12) Otsuka, S.; Nakamura, A.; Tatsuno, Y. *J. Am. Chem. Soc.* **1969**, 91, 6994.
- (13) Brown, M. P.; Puddephatt, R. J.; Rashidi, M.; Seddon, K. R. *J. Chem. Soc., Dalton Trans.* **1977**, 951.
- (14) Brown, M. P.; Puddephatt, R. J.; Rashidi, M.; Seddon, K. R. *J. Chem. Soc., Dalton Trans.* **1978**, 1540.
- (15) Xu, Q.; Heaton, B. T.; Jacob, C.; Mogi, K.; Ichihashi, Y.; Souma, Y.; Kanamori, K.; Eguchi, T. *J. Am. Chem. Soc.* **2000**, 122, 6862.
- (16) Bennett, M. A.; Bhargava, S. K.; Privér, S. H.; Willis, A. C. *Eur. J. Inorg. Chem.* **2008**, 3467.
- (17) Deacon, G. B.; Nelson-Reed, K. T. *J. Organomet. Chem.* **1987**, 322, 157.
- (18) Deacon, G. B.; Elliott, P. W.; Erven, A. P.; Meyer, G. Z. *Anorg. Allg. Chem.* **2005**, 631, 843.
- (19) Wisner, J. M.; Bartczak, T. J.; Ibers, J. A.; Low, J. L.; Goddard, W. A., III. *J. Am. Chem. Soc.* **1986**, 108, 347.
- (20) Wisner, J. M.; Bartczak, T. J.; Ibers, J. A. *Organometallics* **1986**, 5, 2044.
- (21) Albano, V.; Bellon, P. L.; Scatturin, V. *J. Chem. Soc., Chem. Commun.* **1966**, 507.
- (22) Chaloner, P. A.; Hitchcock, P. B.; Broadwood-Strong, G. T. L. *Acta Crystallogr., Sect. C* **1989**, 45, 1309.
- (23) The coordination geometry of [Pd(PPh₃)₃] has been described as a strongly flattened trigonal pyramid with the Pd atom 0.160 Å above the P₃ plane: Stromnova, T. A.; Sergienko, V. S.; Kisin, A. V.; Porai-Koshits, M. A.; Moiseev, I. I. *Bull. Acad. Sci. USSR, Div. Chem. Sci. (Engl. Transl.)* **1987**, 36, 821.
- (24) Fong, S.-W. A.; Evans, K.; Henderson, W.; Nicholson, B. K.; Hor, T. S. A. *Inorg. Chim. Acta* **2010**, 363, 301.
- (25) Barnes, N. A.; Brisdon, A. K.; Fay, J. G.; Pritchard, R. G.; Warren, J. E. *Inorg. Chim. Acta* **2005**, 358, 2543.
- (26) Arnold, D. P.; Bennett, M. A.; McLaughlin, G. M.; Robertson, G. B.; Whittaker, M. J. *J. Chem. Soc., Chem. Commun.* **1983**, 32.
- (27) Allen, E. A.; Wilkinson, W. *Spectrochim. Acta* **1974**, 30A, 1219.
- (28) Goggin, P. L. *J. Chem. Soc., Dalton Trans.* **1974**, 1483.
- (29) For example: [PdMe₂(TMEDA)] [2.026(3) Å],³⁰ *trans*-[Pd(Me)(OPh)(PMe₃)₂·PhOH] [2.039(4), 2.044(5) Å],³¹ *trans*-[Pd(Me)(OCO₂H)(PEt₃)₂] [2.05(2) Å],³² *trans*-[Pd(Et)Br(PMe₃)₂] [2.063(5) Å],³³ [PdMe₂(dmpm)] [2.088(4) Å],³⁰ and *cis*-[PdMe₂(PMePh₂)₂] [2.089(3), 2.090(3) Å].^{18,19}
- (30) de Graaf, W.; Boersma, J.; Smits, W. J. J.; Spek, A. L.; van Koten, G. *Organometallics* **1989**, 8, 2907.
- (31) Kim, Y. J.; Osakada, K.; Takenaka, A.; Yamamoto, A. *J. Am. Chem. Soc.* **1990**, 110, 1096.
- (32) Crutchley, R. J.; Powell, J.; Faggiani, R.; Lock, C. J. L. *Inorg. Chim. Acta* **1977**, 24, L15.
- (33) Osakada, K.; Ozawa, Y.; Yamamoto, A. *J. Chem. Soc., Dalton Trans.* **1991**, 759.
- (34) An apparent Pd–Me distance of 2.28(4) Å has been reported for the A-frame complex [Pd₂(μ-I)(I)(Me)(μ-dppm)₂]BF₄·0.5H₂O as a result of 50% disorder between terminal iodide and methyl ligands: Olmstead, M. M.; Farr, J. P.; Balch, A. L. *Inorg. Chim. Acta* **1981**, 52, 47.
- (35) Bennett, M. A.; Bhargava, S. K.; Ke, M.; Willis, A. C. *J. Chem. Soc., Dalton Trans.* **2000**, 3537.
- (36) Werner, H. *Adv. Organomet. Chem.* **1981**, 19, 155, and references therein.
- (37) Murahashi, T.; Kurosawa, H. *Coord. Chem. Rev.* **2002**, 231, 207, and references therein.
- (38) Maitlis, P. M.; Espinet, P.; Russell, M. J. H. In *Comprehensive Organometallic Chemistry*; Wilkinson, G., Stone, F. G. A., Abel, E. W., Eds.; Pergamon: Oxford, 1982; Vol. 6, p 265.
- (39) Dixon, K. R.; Dixon, A. C. In *Comprehensive Organometallic Chemistry II*; Abel, E. W.; Stone, F. G. A.; Wilkinson, G., Eds.; Pergamon: Oxford, 1995; Vol. 9, p 193.
- (40) Canty, A. J. In *Comprehensive Organometallic Chemistry II*; Abel, E. W.; Stone, F. G. A.; Wilkinson, G., Eds.; Pergamon: Oxford, 1995; Vol. 9, p 226.
- (41) For example: (a) Barder, T. *J. Am. Chem. Soc.* **2006**, 128, 898. (b) Han, X.; Weng, Z.; Hor, T. S. A. *J. Organomet. Chem.* **2007**, 692, 5690. (c) Proutiere, F.; Aufiero, M.; Schoenebeck, F. *J. Am. Chem. Soc.* **2012**, 134, 606. (d) Aufiero, M.; Proutiere, F.; Schoenebeck, F. *Angew. Chem., Int. Ed.* **2012**, 51, 7226.
- (42) Young, S. J.; Kellenberger, B.; Reibenspies, J. H.; Himmel, S. E.; Manning, M.; Anderson, O. P.; Stille, J. K. *J. Am. Chem. Soc.* **1988**, 110, 5744.
- (43) Rashidi, M.; Vittal, J. J.; Puddephatt, R. J. *J. Chem. Soc., Dalton Trans.* **1994**, 1283.
- (44) Benner, L. S.; Balch, A. L. *J. Am. Chem. Soc.* **1978**, 100, 6099.
- (45) Guimerans, R. R.; Balch, A. L. *Inorg. Chim. Acta* **1983**, 22, L177.
- (46) Farr, J. P.; Wood, F. E.; Balch, A. L. *Inorg. Chem.* **1983**, 22, 3387.
- (47) Párkányi, L.; Szalontai, G.; Besenyei, G. *Inorg. Chim. Acta* **2006**, 359, 2933.
- (48) Anderson, G. K.; Kumar, R. *Inorg. Chim. Acta* **1985**, 97, L21.
- (49) Balch, A. L.; Hunt, C. T.; Lee, C. L.; Olmstead, M. M.; Farr, J. P. *J. Am. Chem. Soc.* **1981**, 103, 3764.
- (50) Puddephatt, R. *J. Chem. Soc. Rev.* **1983**, 12, 99.
- (51) Bennett, M. A.; Bhargava, S. K.; Mirzadeh, N.; Privér, S. H.; Wagler, J.; Willis, A. C. *Dalton Trans.* **2009**, 7537.
- (52) Sakamoto, M.; Shimizu, I.; Yamamoto, A. *Chem. Lett.* **1995**, 12, 1101.
- (53) Kwong, F. Y.; Lai, C. M.; Lu, M.; Chan, K. S. *Tetrahedron* **2004**, 60, 5635.
- (54) Penno, D.; Lillo, V.; Koshevoy, I. O.; Sanaú, M.; Ubeda, M. A.; Lahuerta, P.; Fernández, E. *Chem.—Eur. J.* **2008**, 14, 10648.
- (55) Ugo, R.; Cariati, F.; La Monica, G. *Inorg. Synth.* **1968**, 11, 195.
- (56) Coulson, D. R. *Inorg. Synth.* **1990**, 28, 107.
- (57) Kemmitt, R. D. W.; McKenna, P.; Russell, D. R.; Sherry, L. J. *J. Chem. Soc., Dalton Trans.* **1985**, 259.
- (58) Tatsuno, Y.; Yoshida, T.; Otsuka, S. *Inorg. Synth.* **1990**, 28, 342.
- (59) Green, M.; Howard, J. A. K.; Murray, M.; Spencer, J. L.; Stone, F. G. A. *J. Chem. Soc., Dalton Trans.* **1977**, 1509.
- (60) Ogoshi, S.; Morita, M.; Inoue, K.; Kurosawa, H. *J. Organomet. Chem.* **2004**, 689, 662.
- (61) Dell'Amico, D. B.; Labella, L.; Marchetti, F.; Samaritani, S. *J. Organomet. Chem.* **2011**, 696, 1349.
- (62) gNMR (version 5.1) for Windows; Cherwell Scientific Publishing.
- (63) SMART software (version 5.625) for the CCD Detector System; Bruker AXS Inc.: Madison, WI, 2001.
- (64) SAINTPLUS software (version 6.22) for the CCD Detector System; Bruker AXS Inc.: Madison, WI, 2001.
- (65) Blessing, R. H. *Acta Crystallogr., Sect. A* **1995**, 51, 33.
- (66) Sheldrick, G. M. *SHELXTL* (version 6.10); University of Göttingen, Germany, 1994.
- (67) COLLECT Software; Nonius-BV: Delft, The Netherlands, 1997–2001.
- (68) Otwinowski, Z.; Minor, W. In *Methods in Enzymology*; Carter, C. W., Jr.; Sweet, R. M., Eds.; Academic Press, 1997; Vol. 276, pp 307–326.

(69) SIR92: Altomare, A.; Cascarano, G.; Giacovazzo, C.; Guagliardi, A.; Burla, M. C.; Polidori, G.; Camalli, M. *J. Appl. Crystallogr.* **1994**, *27*, 435.

(70) Betteridge, P. W.; Carruthers, J. R.; Cooper, R. J.; Prout, K.; Watkin, D. J. *J. Appl. Crystallogr.* **2003**, *36*, 1487.

(71) *International Tables for X-ray Crystallography*; The Kynoch Press: Birmingham, England, 1974; Vol. IV.

(72) *International Tables for X-ray Crystallography*; Kluwer Academic: Boston, MA, 1992; Vol C.

(73) Krannich, L. K.; Kanjolia, R. K.; Watkins, C. L. *Magn. Reson. Chem.* **1987**, *25*, 320.